

Impact of multiple component deterioration and exposure conditions on seismic vulnerability of concrete bridges

Jayadipta Ghosh* and Jamie E. Padgett

Department of Civil and Environmental Engineering, Rice University, Houston, Texas 77005, USA

(Received February 10, 2011, Revised December 11, 2011, Accepted January 3, 2012)

Abstract. Recent studies have highlighted the importance of accounting for aging and deterioration of bridges when estimating their seismic vulnerability. Effects of structural degradation of multiple bridge components, variations in bridge geometry, and comparison of different environmental exposure conditions have traditionally been ignored in the development of seismic fragility curves for aging concrete highway bridges. This study focuses on the degradation of multiple bridge components of a geometrically varying bridge class, as opposed to a single bridge sample, to arrive at time-dependent seismic bridge fragility curves. The effects of different exposure conditions are also explored to assess the impact of severity of the environment on bridge seismic vulnerability. The proposed methodology is demonstrated on a representative class of aging multi-span reinforced concrete girder bridges typical of the Central and Southeastern United States. The results reveal the importance of considering multiple deterioration mechanisms, including the significance of degrading elastomeric bearings along with the corroding reinforced concrete columns, in fragility modeling of aging bridge classes. Additionally, assessment of the relative severity of exposure to marine atmospheric, marine sea-splash and deicing salts, and shows 5%, 9% and 44% reduction, respectively, in the median value bridge fragility for the complete damage state relative to the as-built pristine structure.

Keywords: seismic fragility; bridge class; aging; corrosion; probability

1. Introduction

Many existing highway bridges in the United States are located in regions characterized by moderate to high seismicity (FHWA 2009). In addition to the seismic hazard, these bridges are further threatened by the ill effects of aging and deterioration due to proximity to harsh environmental conditions. Hence evaluation of seismic vulnerability of highway bridges should also take into account the time evolving loss of structural capacity because an aging bridge is naturally expected to be more vulnerable to seismic shaking. In this context, recent studies that assess the vulnerability of these key elements of the transportation network recognize the importance of capturing such multi-hazard threats. One of the most prevalent ways adopted by researchers to portray the seismic vulnerability of pristine or aging highway bridges has been through the use of bridge fragility curves, which are conditional probability statements that quantify the probability of bridge failure given the intensity of ground motion (Basoz and Kiremidjian 1999, Choe *et al.* 2008,

*Corresponding author, Graduate Student, E-mail: jayadipta.ghosh@rice.edu

Ghosh and Padgett 2010, Nielson and DesRoches 2007a, Shinozuka *et al.* 2000).

Recent studies on the seismic fragility of aging bridges typically show that there is an increase in vulnerability along the service life of the bridge. For instance, Choe *et al.* (2008, 2009) has highlighted the reduced capacity and increased fragility of a typical aging single-bent bridge in California in marine splash zone while focusing only on the corrosion deterioration of reinforced concrete (RC) bridge columns. Corrosion deterioration has been identified as a primary form of deterioration in highway bridges that leads to the cross-sectional area loss of steel and secondary effects such as cracking and spalling of concrete cover (Choe *et al.* 2008, Zhong *et al.* 2011). Additionally, though not considered in this study, corrosion can also potentially lead to changes in mechanical characteristics of steel as identified by Maslehuddin *et al.* (1990) and Almusallam (2001). However, although such instances of approximating aging bridge vulnerability based on corrosion deterioration of a single bridge component may be reasonable for integral frame bridges, the same may not be true for bridges where bearings separate the superstructure and substructure. The primary reason behind this is twofold. Firstly, seismically vulnerable bridge bearings are often found to contribute significantly to the seismic fragility of bridge systems (Nielson and DesRoches 2007b). Secondly, bridge bearings are significantly vulnerable to adverse environmental conditions such as increase in stiffness of rubber bearings due to thermal oxidation and sectional loss of steel in anchor bolts and dowel bars (Silano and Brinckerhoff 1993, Lindquist 2008, Itoh and Gu 2009a, Ghosh and Padgett 2010). Concrete girder bridges typically employ fixed and expansion type elastomeric bearings consisting of a neoprene rubber pad and steel dowels connecting the superstructure and substructure. These elastomeric bearings have been found to perform better under seismic shaking as compared to steel bearings, but are prone to 'walking out' from under the girder under large deformations (Imbsen and Nutt 1981, Nielson 2005). Additionally, the performance of these bearings is also affected due to aging and deterioration. For instance, Itoh and Gu (2009) conducted several laboratory experiments under accelerated thermal oxidation conditions and showed that natural rubber bridge bearings undergo significant changes in material properties (such as stiffness, shear modulus, etc.) with time under normal in-field service conditions. Moreover, similar to the degradation mechanism of reinforcing steel in RC columns, the dowel bars in elastomeric bridge bearings are also expected to corrode due to chloride ingress through the concrete cover. Hence, a primary focus of this research is to inspect the deterioration mechanisms and subsequent impact on seismic fragility of such concrete bridge classes with multiple deteriorating bridge components, not investigated till date to the authors' knowledge.

Since prior conclusions on the significance of aging in seismic fragility modeling have been based upon studies of single bridge samples (Choe *et al.* 2008, 2009, Ghosh and Padgett 2010), variation in bridge geometry is considered in this study while assessing the detrimental effects of aging on the seismic vulnerability of classes of bridges. This study evaluates time dependent fragility curves for a class of multi-span simply supported (MSSS) concrete bridges typical of the Central and Southeastern US (CSUS), considering the inherent variations in bridge geometry expected in a class of structures. Additional uncertainties in material properties, modeling parameters and deterioration parameters are also propagated in deriving the component and system fragility curves following the nonlinear dynamic analyses of the analytical bridge models. Evaluation of time evolving fragility curves for such bridge classes will help to evaluate the vulnerability of spatially distributed bridges under seismic hazards. To assess the impact of severity of the environment on the deterioration and seismic behavior of critical bridge components, aging bridge fragility curves for these bridge classes are also derived for different deterioration exposure

conditions. The exposure conditions considered in this study include exposure to chlorides from two sources: deicing salt exposure and marine exposure. Furthermore, under marine exposure two different scenarios are considered, namely, the splash zone and atmospheric zone. Finally, time dependent polynomial regression functions are proposed that helps to assess the impact of a specific exposure condition on the bridge class fragility along its service life. These scaling factors can be applied to approximate the effects of deterioration on the seismic fragility curves for reinforced concrete girder bridge classes used in risk assessment.

2. Deterioration mechanisms for reinforced concrete girder bridges

Primary reasons for loss of strength of lateral force resistance in bridge components can be attributed to factors such as corrosion, erosion, other forms of chemical deterioration and fatigue (Melchers and Frangopol 2008). Hence, the structural resistance of bridge components is a time-evolving parameter that may decrease along the structure's service life and thereby affect the dynamic response and fragility under seismic loads. The sections below discuss the deterioration mechanisms adopted for two critical bridge components: reinforced concrete columns and elastomeric bridge bearings. Characterizing these deterioration mechanisms and capturing their potential uncertainties will help to assess the seismic behavior and fragility of aging bridge components and overall bridge system. The extent of impact of aging mechanisms on the seismic vulnerability of concrete bridges will be assessed in details in Sections 4 and 5.

2.1 Deterioration mechanisms for aging bridge columns

A wealth of literature exists on the corrosion deterioration mechanism of reinforcing steel embedded in concrete, which is typically represented by Fick's second law of diffusion through a semi-infinite solid (Stewart and Rosowsky 1998). The concentration of chloride ions in concrete must however reach a critical threshold to dissolve the protective passive film around the reinforcement, thus initiating reinforcement corrosion. The corrosion initiation time is found to typically depend on the environmental exposure condition. The exposure conditions considered in this research include exposure to chlorides from deicing salts and marine exposure (both splash zone and atmospheric zone).

It has been shown by researchers that deicing salt exposure results in constant chloride ion concentration near the concrete surface (Hoffman and Weyers 1996, Vu and Stewart 2000) and the corresponding corrosion initiation time is given by (Thoft-Christensen *et al.* 1996)

$$T_{i_{deicing}} = \frac{x^2}{4D_c} \left[\operatorname{erf}^{-1} \left(\frac{C_0 - C_{cr}}{C_0} \right) \right]^2 \quad (1)$$

where, $T_{i_{deicing}}$ is the corrosion initiation time due to deicing salt exposure, x is the concrete cover depth, D_c is the chloride diffusion coefficient, C_0 is the equilibrium chloride concentration at the concrete surface, C_{cr} is the critical chloride concentration that causes dissolution of the protective passive film around the reinforcement and initiates corrosion and erf is the Gaussian error function. Corrosion initiation time for RC members located in marine splash and atmospheric zones under the exposure of chlorides can be estimated based on Eq. (2) (Bertolini *et al.* 2004, Choe *et al.* 2009)

$$T_{i_{marine}} = \left\{ \frac{xR_{cl,0}}{4k_c k_e(t_0)^{n_{cl}}} \left[\operatorname{erf}^{-1} \left(1 - \frac{C_{cr}}{C_0} \right) \right]^2 \right\}^{\frac{1}{(1-n_{cl})}} \quad (2)$$

where, $R_{cl,0}$ is the chloride penetration resistance (inverse of chloride diffusion coefficient) determined from compliance tests, k_c is the curing factor, k_e is the environmental factor, t_0 is the age of concrete when the compliance test is performed, n_{cl} is the age exponent that incorporates the densification of cement paste due to further hydration.

Once corrosion initiates by either chloride exposure from deicing salts or marine exposure, the time dependent loss of reinforcement cross-sectional area can be calculated using the diameter of pristine longitudinal rebar and rate of metal loss due to corrosion (Thoft-Christensen *et al.* 1996, Enright and Frangopol 1998). In some instances, the corrosion rate has been considered by researchers as a constant parameter along the service life primarily due to lack of explicit data for time dependent corrosion rate modeling (Frangopol *et al.* 1997, Val *et al.* 2000, Akgul and Frangopol 2004, Liu 2005). However, limited accelerated corrosion tests in the laboratory by researchers have shown the potential time dependence of corrosion current density. For instance, Eq. (3) shows the commonly adopted form of corrosion current density (in $\mu A/cm^2$) at the beginning of corrosion propagation phase of RC structures (Yokozaki *et al.* 1997, Vu and Stewart 2000). Subsequently, based on limited laboratory experiments, Vu and Stewart (2000) observed that this initial corrosion current density reduces with time following Eq. (4).

$$i_{corr_0} = \frac{37.8(1-w/c)^{-1.64}}{x} \quad (3)$$

$$i_{corr}(t) = 0.85 i_{corr_0} (t - T_{i_{marine}})^{-0.29} \quad (4)$$

In the above equations, i_{corr_0} is the initial corrosion current density, $i_{corr}(t)$ is corrosion current density at time t in the service life of the aging bridge component, w/c is the water cement ratio of concrete and x is the cover depth in mm. Both i_{corr_0} and $i_{corr}(t)$ can be multiplied with suitable conversion factors to arrive at the corresponding corrosion rates (r_{corr}). In this paper the time dependent model is considered for chlorides stemming from marine exposure conditions and in the absence of validated time-varying models for deicing salt exposure a more simplified model of a constant rate of corrosion is adopted.

The probabilistic loss of steel area due to corrosion deterioration is modeled as a reduction in longitudinal reinforcement bar cross-sectional area in the fiber section finite element bridge model as described in later sections. Additionally, it should be noted that corrosion deterioration and corresponding loss of steel area might also lead to potential secondary effects such as cracking and spalling of cover concrete. This phenomenon is incorporated in this study by adopting the model proposed by Duracrete (2000). It is also noted that complete cover loss could lead to potential buckling of longitudinal reinforcement during seismic events. However, a preliminary investigation shows that even under severe deterioration conditions, explicit incorporation of rebar buckling phenomena in the bridge models results in less than 1% shift in fragility estimates. Consequently, rebar buckling phenomena is not considered in the finite element aging bridge models. Another secondary effect of corrosion, not considered in this study is the loss of bond strength between steel

and concrete due to corrosion. While previous studies have shown that loss of bond strength is significant for unconfined RC members (Fang *et al.* 2004, Aquino and Hawkins 2007), it is negligible for members with transverse confinement (Fang *et al.* 2004). Following the provisions for pre-seismic detailing, bridge columns in CSUS are modestly confined and hence fall in between the two above mentioned categories. Deficiencies in experimental data for columns with limited confinement underline the need for future work in this area of research that will lead to viable improvement of analytical models. The studies herein hence focus on the effects of area loss of reinforcing steel and consequent cracking and spalling of concrete in the RC columns.

2.2 Deterioration mechanisms for aging elastomeric bearings

The primary function of elastomeric bridge bearings is the transfer of forces from the concrete girder superstructure to the substructure. These bearing assemblies consist of two components: an elastomeric rubber pad and steel dowels for restraint as shown in Fig. 1(a). Each individual component of this type of bearing assembly plays a unique role in the transfer of forces from the superstructure to the columns. For instance, the elastomeric pad transfers lateral forces by developing frictional forces, while the steel dowels offer resistance through a beam type action (Taylor 1969). Consequently, Choi (2002) and Nielson (2005) developed individual analytical models for each of these components and combined them in parallel to achieve the composite action. The elastomeric bearing assembly can be of fixed or expansion type depending on the size of the slot in the bearing pad as shown in Fig. 1(b). Analogous to the mechanical modeling approach, the deterioration mechanisms for the bearing assembly can be divided into the degradation of the elastomeric bearing pad due to thermal oxidation leading to an increase in shear

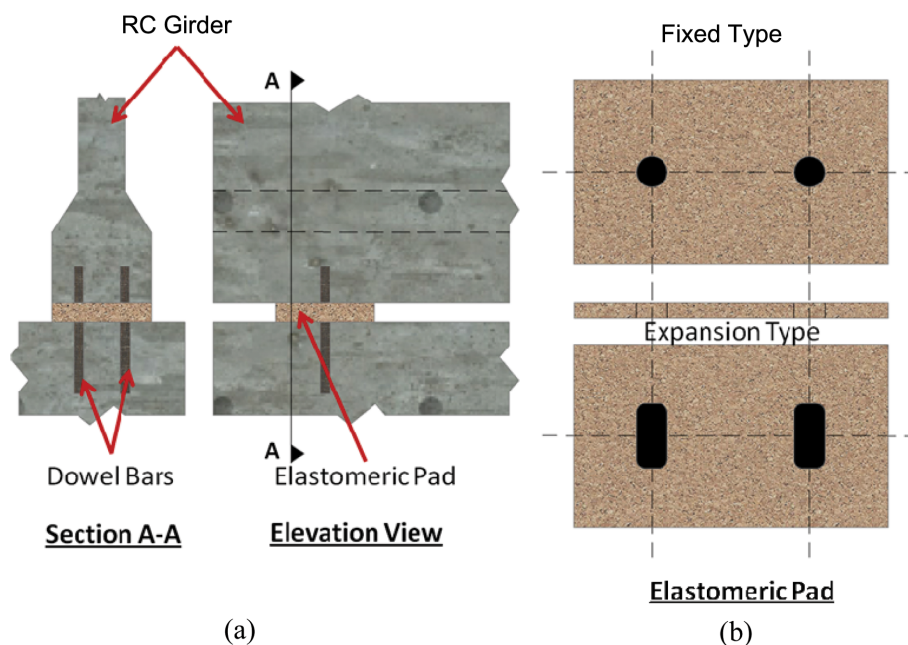


Fig. 1 (a) Elevation and section view of elastomeric pad bearings used for concrete bridge girders and (b) fixed and expansion bearings types depending on dimensions of the slot

stiffness and the area loss of steel dowels due to corrosion attacks as elaborated in the following sections.

A key element in the analytical modeling of elastomeric pads lies in the determination of initial shear stiffness of the pad which can be expressed as (Kelly 1997, Choi 2002)

$$k_i = \frac{GA_{pad}}{t_{pad}} \quad (5)$$

where, G is the shear modulus of the rubber, A_{pad} is the area of the elastomeric bearing pad and t_{pad} is the thickness. Typically a mean value of the shear modulus based on AASHTO recommendations is assumed in analytical modeling and seismic fragility analyses of bridges with elastomeric bearings. However, following a series of accelerated exposure tests Itoh *et al.* (2006) concluded that the shear modulus of rubber, amongst other properties, is not constant and is highly affected by degradation mechanisms such as thermal oxidation. Consequently, Itoh and Gu (2009b) proposed an aging model for natural rubber bearings that reflects the relation among the variation of the different material properties of rubber bearings with temperature, and aging time. For instance they proposed that under accelerated exposure test conditions the variation in strain energy due to thermal oxidation can be given by

$$\frac{SE_s}{SE_0} = c_s \sqrt{t_{aging}} + 1 \quad (6)$$

where SE_s/SE_0 is the relative strain energy as compared to the initial state at the rubber surface at a specific value of uniaxial strain, SE_0 being the strain energy at the initial state for the same value of uniaxial strain, c_s is the temperature dependent coefficient for strain energy and t_{aging} is the aging time at test temperature in hours under accelerated test conditions.

As evident from Eq. (6), this formulation is valid only for aging times at the selected test temperature and hence there is a need to correlate the accelerated aging results with deterioration under in-field service conditions at alternate temperatures. This correlation can be achieved using the Arrhenius methodology in the formula proposed by Le Huy and Evrard (1998) as

$$\ln\left(\frac{t_{test}}{t_{field}}\right) = \frac{E_a}{R} \left(\frac{1}{T_{test}} - \frac{1}{T_{field}} \right) \quad (7)$$

where, t_{field} is the time of exposure of the rubber bearing in the field, E_a is the activation energy of rubber, R is the gaseous constant, T_{test} is the absolute temperature under accelerated thermal oxidation test and T_{field} is the absolute temperature in the field service conditions.

The measure of strain energy change as given by Eq. (6) can also be used to measure a change in shear modulus (G) to estimate the updated value of initial shear stiffness k_i of the bearing pad for use in fragility modeling of aging bridges. This change can be measured by using a one-parameter *neo-Hookean* material model which provides a simple relation between strain energy and the shear modulus expressed as (Mase and Mase 1999)

$$SE = G \left(\lambda^2 + \frac{2}{\lambda} - 3 \right) \quad (8)$$

where, SE is the strain energy, G is the shear modulus and λ is a measure of uniaxial strain for the rubber specimen. Hence a relative change in shear modulus of the rubber bearing due to aging can simply be measured from change in the value of strain energy as follows

$$\frac{G_{aging}}{G_0} = \frac{SE_s}{SE_0} \quad (9)$$

where, G_{aging} is the shear modulus of the aging rubber bearing at time $t = t_{field}$, and G_0 is the initial assumed strain energy at time t_0 . The ratio SE_s/SE_0 can be conveniently calculated from Eq. (6) as presented earlier for the accelerated thermal oxidation tests, and shear modulus of the aging bearing derived from Eq. (9).

In addition to the stiffening of bearing pad due to thermal oxidation, environmental deterioration mechanisms such as corrosion deterioration leads to area loss of steel dowel bars and thereby weakens the performance of the bearing assembly. This corrosion process primarily results from leakage of chloride laden saltwater through malfunctioning deck joints. Additionally the chloride induced deterioration process of bearing dowels may be further exacerbated from high level of horizontal stresses induced in bridge bearings during seismic events (Silano and Brinckerhoff 1993). The scope of the present study is limited to corrosion resulting only from chloride induced deterioration and the area loss deterioration mechanism is similar to that adopted for reinforcing steel in RC columns outlined in the previous sections in Eqs. (1) to (4).

3. Overview of fragility methodology and description of aging case study bridge class

The preceding section on deterioration of bridge components indicates that the structural resistance and modeling parameters of these components are not constant. Consequently, the probability of failure of the bridge components and hence the overall bridge system fragility is also a time evolving parameter. This section elaborates on the approach to develop time dependent bridge fragility curves for aging bridge classes and is followed by introduction of the case study concrete bridge class in Central and Southeastern US adopted for demonstration purposes.

3.1 Time-evolving bridge fragility curves

Fragility curves can be best described as conditional probability statements that provide an estimate of the probability of bridge component or system failure given the intensity of ground motion. Mathematically, the time-dependent fragility of the m^{th} bridge component can be represented as

$$P_{fm}(t) = P[D_m(t) > C_m(t) | IM] \quad (10)$$

where, $D_m(t)$ is the demand placed on bridge component m at time t , while $C_m(t)$ is the capacity of the component at the same instant of time and IM is the intensity of ground motion.

As shown in Eq. (10), the seismic fragility analysis requires probabilistic estimates of both the demand placed upon and structural capacity of deteriorating bridge components. Probabilistic

seismic demand models (PSDMs) at each point in time along the service life of the bridge are generated following the power law relation proposed by Cornell *et al.* (2002) that relates the median of the seismic demand (S_{d_m}) with the intensity of ground motion (IM). When presented in a time-dependent format for aging bridges, this relation follows the form as

$$S_{d_m}(t) = a(t)IM^{b(t)} \quad (11)$$

where, $a(t)$ and $b(t)$ are the regression parameters which will change depending on the level of deterioration and hence the point in time in the service life of the bridge class. The probabilistic seismic demands for bridge components are constructed after conducting nonlinear time history analyses of bridge samples considering uncertainty in several parameters such as bridge class geometry, ground motion characteristics, material properties, modeling parameters and deterioration variables. The seismic demand response parameters chosen in this study for the different bridge components are presented in Table 1.

The limit states for slight, moderate, extensive and complete damage used in this study (Table A1 in appendix A) are adopted from Nielson and DesRoches (2007b) and are based on a statistical combination of experimental results and expert judgment. Although the adopted limits state capacities are not assumed to change directly throughout the life of the bridge, the effects of aging and deterioration are implicitly incorporated through either the normalization or through the bridge modeling which renders achieving of the displacements easier due to changes in stiffness or yield strength. For instance, for components such as deteriorated bridge columns, the effects of corrosion on column capacity are incorporated while calculating the curvature ductility demand ratio as a measure of seismic demand. The ductility demand ratio expressed as

$$\mu_\phi = \frac{\phi_{\max}}{\phi_{\text{yield}_{\text{corroded}}}} \quad (12)$$

where, ϕ_{\max} is the maximum curvature demanded on the column and $\phi_{\text{yield}_{\text{corroded}}}$ is the curvature at which the first yield of the outermost corroding reinforcing bar occurs (Ghosh and Padgett 2010).

Additionally, limit states for the bearing deformations were obtained by Nielson and DesRoches (2007a) following Bayesian updating of experimentally observed capacity estimates with results from a functionality based survey conducted by Padgett and DesRoches (2007). Since these limit states are based on offsets at joints, or relative displacements between the bridge superstructure and

Table 1 Bridge component response parameters and abbreviations used in this study

Component	Response parameter	Abbreviation
Column response	Curvature ductility	μ_ϕ
Fixed bearing longitudinal response	Deformation	FBL
Fixed bearing transverse response	Deformation	FBT
Expansion bearing longitudinal response	Deformation	EBL
Expansion bearing transverse response	Deformation	EBT
Abutment active response	Deformation	AA
Abutment passive response	Deformation	AP
Abutment transverse response	Deformation	AT

substructure, they are not affected by the level of corrosion deterioration. However they may be rendered easier to achieve in the models through the loss of doweling. In all cases, the time dependent effects of deterioration are incorporated in the analytical models of the bearings through a reduction in ultimate lateral strength of the bearing due to corrosion of dowel bars and also through increasing shear stiffness of bearing pads due to thermal oxidation. Future experimental studies on capacity estimates for deteriorating structures can further lead to improved fragility estimates for aging bridge components and bridge systems.

Both the seismic demands and capacity limit state estimates of different bridge components are often expressed in terms of lognormal distributions (Choi *et al.* 2004, Nielson and DesRoches 2007a, Padgett and DesRoches 2008) as adopted in this study. The bridge component fragilities therefore follow a closed form solution given by

$$P_{f_m}(t) = \Phi\left(\frac{\ln(IM) - \ln(\text{med}_m(t))}{\text{disp}_m(t)}\right) \quad (13)$$

where, $\text{med}_m(t)$ and $\text{disp}_m(t)$ are respectively the time dependent median and dispersion parameters of the lognormal distribution representing the fragility of the m^{th} bridge component. In this approach for deriving time-dependent fragility curves, the median value and dispersion are expressed in terms of the seismic demand and capacity estimates as

$$\text{med}_m(t) = \exp\left[\frac{\ln(S_c) - \ln(a(t))}{b(t)}\right] \quad (14)$$

$$\text{disp}_m(t) = \frac{\sqrt{\beta_D^2(t) + \beta_c^2}}{b(t)} \quad (15)$$

where, S_c and β_c are the median and dispersion of the lognormally distributed component capacity and β_D is the dispersion of the lognormally distributed seismic demand.

To arrive at bridge system level fragilities, a joint probability density function (pdf) for component demands is constructed by estimating the correlation between peak component responses. The bridge system fragility is then evaluated by comparing the joint pdf of demands with the component capacity pdfs for each damage state via Monte Carlo analysis, where the system is approximated as a series system. Thus the system fragility estimates account for component correlations at different points in time along the service life of the bridge. Consequently, the bridge system fragilities can be expressed as

$$P_{f_{\text{sys}}}(t) = \Phi\left(\frac{\ln(IM) - \ln(\text{med}_{\text{sys}}(t))}{\text{disp}_{\text{sys}}(t)}\right) \quad (16)$$

where, $\text{med}_{\text{sys}}(t)$ and $\text{disp}_{\text{sys}}(t)$ are the estimated lognormal parameters of bridge system fragility.

3.2 Aging class of concrete highway bridges

The methodology to determine the time-dependent vulnerability of aging bridge classes presented

in the previous sections is applied to assess the vulnerability of a deteriorating concrete bridge class typical of the Central and Southeastern United States. The bridge class chosen in this study is the non-seismically designed (pre 1990) multi-span simply supported (MSSS) concrete girder bridge which constitutes nearly 19% of all bridges in the region. This bridge type has been identified by previous researchers (Nielson 2005, Nielson and DesRoches 2007) as seismically vulnerable due to inadequate detailing of components. For instance, the columns have insufficient transverse reinforcement consisting of #13 bars spaced at 305 mm on center, inhibiting the shear resistance and ductile capacity. Additionally the elastomeric pad bearings have the potential for ‘walking out’ from under the girders during large deformations in seismic events, and seat widths are inadequate. Furthermore, the reinforcing steel in the concrete columns and the bridge bearings are prone to aging and deterioration. Such mechanisms include corrosion of reinforcing steel in columns and bearing dowel bars along with increase in stiffness of bearing pads due to thermal oxidation as elaborated in the previous sections. For time dependent fragility analysis purposes, eight representative three-span, zero-skew bridges belonging to this particular bridge class are sampled from CSUS bridge inventory. The span lengths, deck widths and column heights of all these eighteen bridges are obtained using Latin Hypercube Sampling techniques from the cumulative

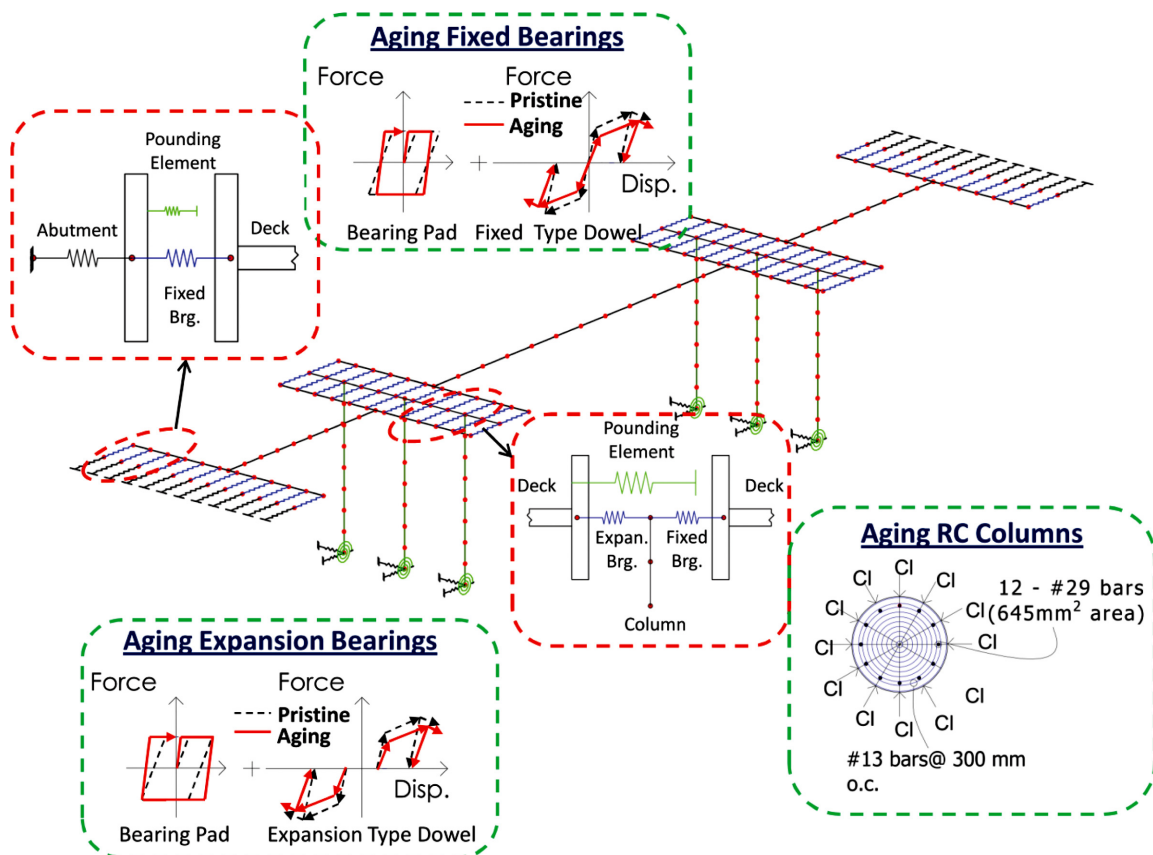


Fig. 2 Typical finite element model of the 3 span MSSS concrete bridge sample showing potential changes in modeling parameters due to aging and deterioration

density functions of span lengths, deck widths and column heights of all such bridges in the inventory. The chosen bridge samples show a variation in mid-span lengths between 6.7 m to 13.2 m, deck widths between 7.7 to 17.9 m and column heights between 4.7 m to 7.3 m. Consequently these statistically chosen bridge samples are paired with a synthetic suite of 96 ground motions developed by Wen and Wu (2001) and Rix and Fernandez (2004) representative of the seismicity of CSUS. Additional uncertainties propagated in the fragility methodology for the MSSS concrete bridge class include material properties, modeling and deterioration parameters.

Fig. 2 shows a typical finite element model of a three span, zero-skew bridge type belonging to the MSSS concrete girder bridge class under consideration. These three dimensional finite element models for each pristine bridge within the bridge class are developed in this study using the finite element software platform OpenSees (Mazzoni *et al.* 2009), following the modeling suggestions by Nielson and DesRoches (2007a). For the deteriorated bridge modeling, in addition to reducing the cross-sectional area of column reinforcement to account for the effects of corrosion deterioration, the figure also shows changes in the force-displacement curves for aging bridge bearing models as compared to the pristine state. The impact of corrosion deterioration of steel members such as reinforced concrete columns, bearing dowel bars and thermal oxidation of the elastomeric bearing pads on the seismic response and fragility of bridge components and system belonging to the bridge class under consideration will be assessed in the following sections.

4. Effects of deterioration mechanisms on bridge components and aging bridge class fragility

In order to understand the impact of component deterioration on bridge class fragility, it is essential to assess how each of these aging components individually affects the bridge response. The component responses in turn depend on the severity of environment, point in time along the service life of the bridge class, and level of degradation of the component under consideration. The primary focus of this section will be to assess component and bridge system performances under corrosion deterioration due to chlorides from deicing salt exposure which has been identified as one of the most severe forms of corrosion (Stewart and Rosowsky 1998). The effects of different exposure conditions other than chlorides resulting from deicing salt on bridge fragilities will be discussed in section 5 of the paper. This section also highlights the changes in the probabilistic seismic demand models of some of the key bridge components when individual component deterioration mechanisms are considered. Finally, fragility curves are presented to evaluate how the vulnerability of the bridge class changes in time for the deicing salt exposure condition which causes deterioration of multiple key components.

4.1 Impact of deterioration mechanisms on critical bridge components

The parameters used to assess the corrosion deterioration of steel members under deicing salt exposure condition are typically assumed to follow lognormal distributions. The probability density distributions for these parameters are shown in Table 2, as identified based on in-field corrosion related studies of bridges under deicing salt exposure in United States (Enright and Frangopol 1998, Ghosh and Padgett 2010, Weyers *et al.* 1994, Whiting *et al.* 1990).

Additionally, to assess the stiffening of the elastomeric bearings, a key input for the Arrhenius

methodology as given in Eq. (7) is the region specific absolute in-field exposure temperature (T_{field}) of these elastomeric pads. The region of interest chosen to assess the exposure to chlorides from deicing salts is the state of Tennessee with an average annual snowfall of 9 inches (in Nashville, capital of Tennessee) and yearly average temperature of 56°F (NOAA 2004, USDOS 2010). The adopted bridge class in this study is assumed to be representative of typical MSSS concrete girder bridges in the state of Tennessee (TN), due to the similarity in design details of bridges across the Central and Southeastern US (Wright *et al.* 2011). Under such conditions, Fig. 3 shows how corrosion deterioration and thermal oxidation manifest in reducing the area of column reinforcing steel and bearing dowel bars while also leading to an increase in horizontal stiffness of the bearing pads. Along with the reduction in the mean value of normalized steel area, Fig. 3(a) also shows the corresponding uncertainty associated at different points in time along the service life of the bridge. Uncertainty associated with increase in shear modulus of the elastomeric bearing pad is considered same as that of the uniformly distributed random variable model adopted by Nielson (2005) for the pristine rubber bearing.

Table 2 Descriptors of lognormal random variables affecting the corrosion deterioration of reinforcement in RC columns and steel dowel bars in elastomeric bridge bearings for the deicing salt exposure condition

Parameter	Unit	Mean	COV*
Cover depth of reinforcing steel in RC columns (x_{RC})	cm	3.81	0.20
Cover depth of dowel bars in bridge bearings (x_{DOW})	cm	5.00	0.20
Surface chloride concentration (C_0)	wt % concrete ⁺	0.10	0.10
Critical chloride concentration (C_{cr})	wt % concrete ⁺	0.040	0.10
Diffusion coefficient (D_c)	cm ² /year	1.29	0.10
Rate of corrosion (r_{corr})	mm/year	0.127	0.3

*COV = Coefficient of variation

⁺wt % concrete = Percent by weight of concrete

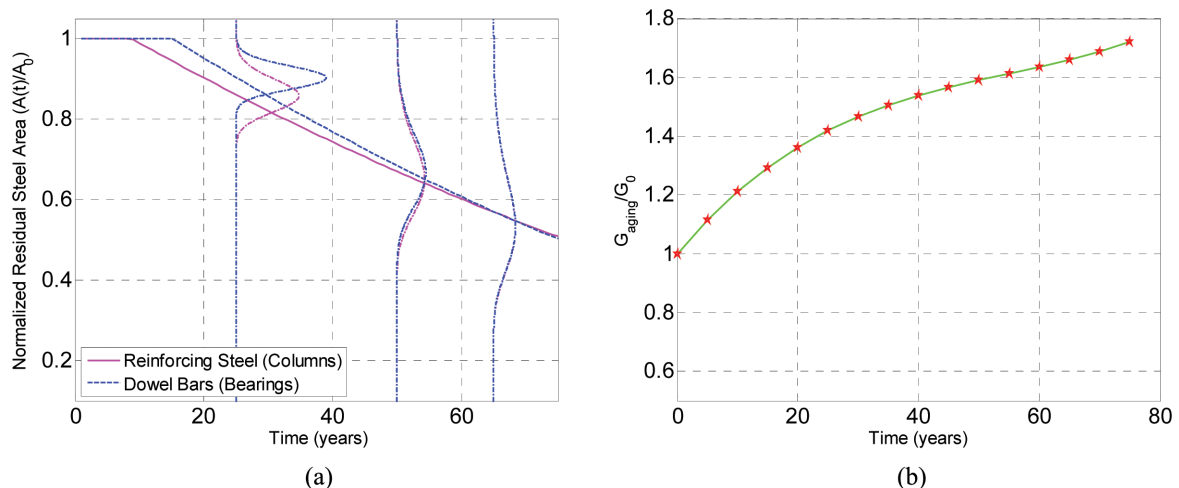


Fig. 3 (a) Normalized cross sectional area reduction of reinforcing steel in RC columns and steel dowels in elastomeric bearings and (b) increase in shear modulus of elastomeric bearing pad

4.2 PSDMs for aging bridge components

Probabilistic seismic demand models of the individual bridge components help to highlight how the seismic demand placed on the components vary under the effects of aging and deterioration. The demand models presented in this section correspond to two points in time in the service life of the bridges (25 years and 50 years) under two distinct scenarios of component deterioration: (a) individual cases of column and bearing deterioration and (b) joint consideration of both degradation effects.

Fig. 4(a) shows the PSDMs for demands placed upon the columns (measured in terms of curvature ductility demand) for the bridge class after 25 and 75 years of exposure to deicing salts. It can be clearly seen in the figure that if only bearing degradation is considered, regardless of the year, it has a negligible impact on the seismic demand placed on the columns. As one would expect, the deterioration of the columns only has a significant influence on the column demand

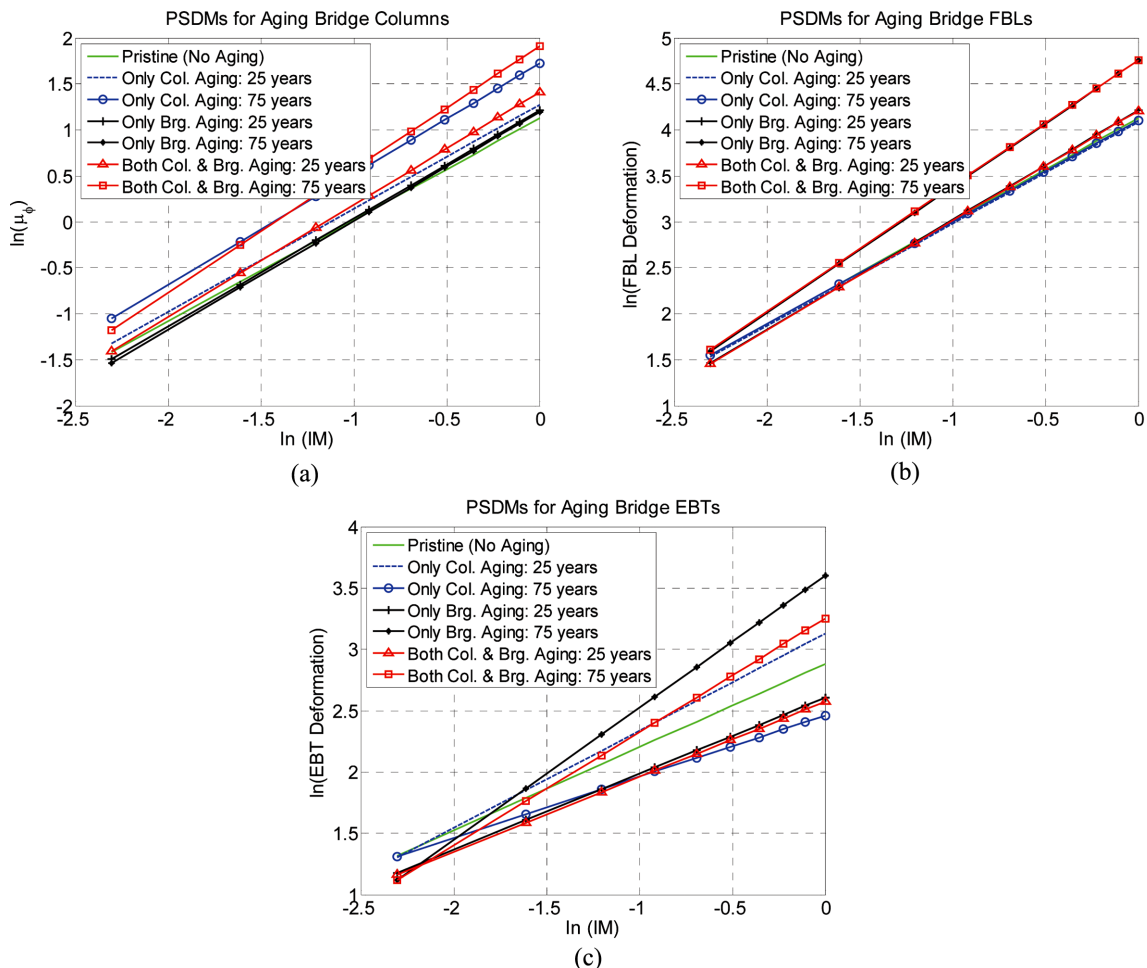


Fig. 4 PSDMs showing median value of demand against intensity measure for (a) RC bridge columns, (b) fixed bearing deformation in the longitudinal direction and (c) expansion bearing deformation in the transverse

which is found to increase steadily with age from 25 to 75 years. Additionally when both column and bearing deteriorations are accounted for, the demands placed on the columns are highest for that particular point in time than when the aging mechanisms are considered individually. Similarly, Fig. 4(b) shows the impact of component deterioration on the response of fixed bearings in the longitudinal direction. Similar to the previous figure this also shows that while only column deterioration has negligible impact on the seismic demand placed on the fixed bearings, bearing degradation has a significant impact in increasing the demand due to aging. In this case however, the joint consideration of these components does not have a significant influence on the demand than when bearing deterioration is considered individually. Additionally, it is misleading to assume that these two individual degradation mechanisms of the columns and bearings have virtually no effect on the response of one another. This is shown in Fig. 4(c) which depicts the PSDMs for the expansion bearings in the transverse direction. This figure shows that initial deterioration of bridge columns at 25 years (under the individual or joint consideration of aging) alone tends to increase the transverse deformation on the expansion bearings, while increased deterioration at 75 years reduces the seismic demand due to the localization of forces and energy dissipation through the heavily deteriorated bridge columns. Similarly, when the effects of bearing deterioration is considered alone, initially at 25 years the effect of increase in horizontal stiffness of bearing pads due to thermal oxidation tends to dominate over the steel area reduction of dowel bars and reduces the transverse displacement of the expansion bearings. However, as the dowel deterioration becomes more pronounced, the deformation and hence the seismic demand placed on the expansion bearings increases far beyond the demands placed on the initial non-deteriorated expansion bearings in the transverse direction.

4.3 Fragility curves for aging MSSS concrete bridge class

Fragility curves are derived for the class of MSSS concrete girder bridges to assess how the joint effects of deterioration of RC columns and elastomeric bridge bearings affect the seismic reliability of key components and the system. In this study fragility curves are developed for four different damage states corresponding to the different limit states previously identified.

Fig. 5 shows the percentage changes in median fragility values of different components (with respect to the pristine bridge) for the slight damage state. A decrease in median value, or negative percent change, reveals an increase in vulnerability to seismic loading; conversely, an increase in median value, or positive percent change, reveals a reduction in seismic vulnerability of the component. The trends in variation of the median fragility parameter for different bridge components as depicted in Fig. 5 are found to remain consistent across all damage states. This figure reveals two interesting trends. Firstly, the median values of certain bridge components, such as bridge columns and fixed bearings in the longitudinal direction, show a consistent decrease (hence an increase in susceptibility to seismic damage) along their service life. On the other hand, both the fixed and expansion bearings in the transverse direction show an initial increase in median values followed by a decrease as the bridge continues to age. This finding is consistent with the assessment of the demand models previously presented. In the initial period, the corrosion of rebars in the columns and dowel bars in the bearings do not have a pronounced effect on the deformation response of these components which is mostly dominated by the stiffening of the elastomeric pad. Additionally, although median values for parameters such as fixed and expansion bearings in the transverse direction show a dramatic increase with a subsequent decrease in median values along

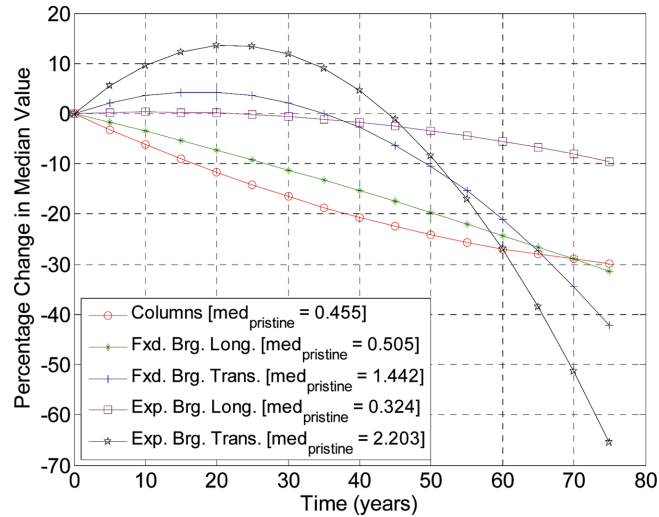


Fig. 5 Percentage change in median fragility values for slight damage state across the service life of different bridge components

the service, the effect of this component on system fragility is negligible owing to its high median value. To further highlight the relative vulnerability of each component at the slight damage state, the median values of the components are shown in the legend of the figure in percent g PGA. It is noted that the relative vulnerability of these components are not consistent across each damage state, although the trends in impact of aging remains similar. Furthermore, while the median values of different bridge components either increase or decrease depending on the point in time along the service life of the bridge, the dispersions are in general found to decrease steadily across all components.

Given the contrasting trends in impact of deterioration on bridge component fragility due to the complex dynamic response of the structure, bridge class fragility curves are developed to quantify the overall impact of aging on system vulnerability. Fig. 6 shows the aging bridge class fragility curves at four different points in time for the moderate and extensive damage states, clearly revealing that aging and deterioration has an overall negative impact on bridge system fragility. This is in contrast to the individual fragilities of some bridge components (Fig. 4) which tend to show a reduced fragility in the initial period of service life, such as the bridge expansion bearings in the transverse direction. This finding underlines the need to consider the effects of multiple bridge component degradation mechanisms while assessing the seismic vulnerability of bridge classes. The results further demonstrate that even after considering uncertainty in ground motion, geometry and modeling parameters the effects of aging and deterioration emerge as critical factors in fragility modeling of the MSSS concrete girder bridge class.

The component and system fragility curves presented in this section for the deicing salt exposure condition are specific to the bridge design and corrosion deterioration parameters specified in Table 2. Since the fragility estimates are significantly dependent on the effects of aging, the deterioration models should be used with caution after a careful assessment of these parameters under consideration. For instance, the cover depth of reinforcing steel in RC Columns (x_{RC}) is a critical parameter affecting the corrosion initiation time and subsequent extent of area loss of steel. In this

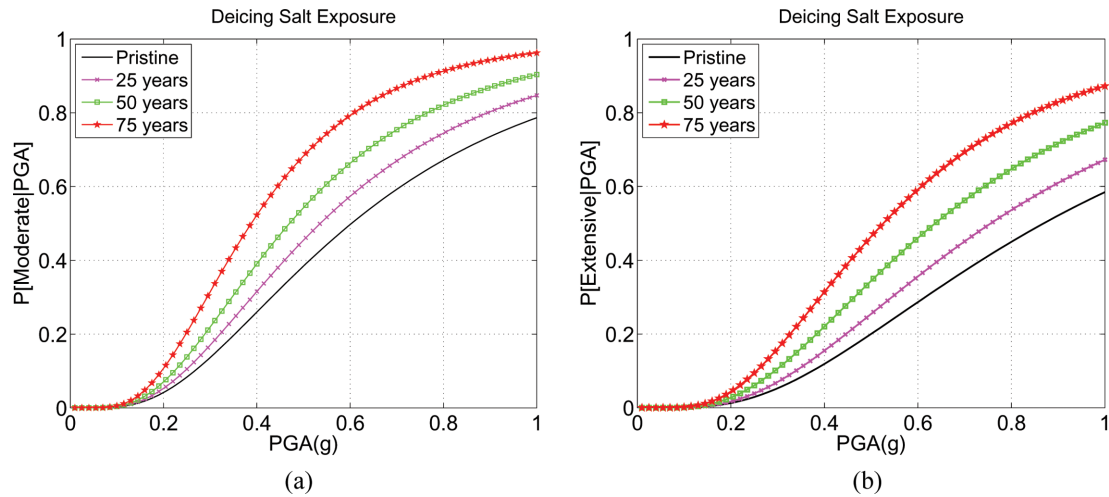


Fig. 6 Fragility curves for MSSS concrete bridge classes for the (a) moderate and (b) extensive damage states under deicing salt exposure

regard, a study conducted by the authors revealed that there is 12% increase in the median fragility values corresponding to the complete damage state for a 75 year old fragility if a mean cover depth of 5.08 cm is used instead of 3.81 cm as considered in this study. Hence, accurate estimates of such parameters should be used to assess the aging bridge fragility estimates. While the focus of this paper till now has been on the deicing salt exposure condition, the seismic performance of the aging MSSS concrete girder bridge given exposure to other sources, such as chlorides from marine splash zones or marine atmospheric zones, is investigated in the next section for comparison.

5. Impact of exposure condition on deteriorated bridge fragility

In addition to the case of deicing salt exposure as elaborated in the preceding section, two additional exposure conditions are considered in this study. These exposure scenarios correspond to proximity to chloride ions stemming from a marine source. Depending on the distance of the bridge structure from the sea coast, the marine exposure condition can further be divided into two scenarios (Davis 2000): (a) sea-splash zone for bridges located very near to the sea coast and subjected to continuous wetting and drying from “splashing” of chloride laden sea water and (b) atmospheric zone for bridges situated away from the coast but subjected to chloride exposure due to salt spray or sea mist blown by the wind from the sea. Consequently, in order to demonstrate the effects of chloride exposure from marine sources, the bridge class under consideration is assumed to be located in the state of South Carolina (SC), which is characterized by moderate seismicity with potential exposure to marine chlorides from the close proximity to the Atlantic Ocean. The probabilistically distributed deterioration parameters to calculate the corrosion initiation time and subsequent area loss of steel embedded in RC members for sea-splash and atmospheric zone can be found in Bertolini *et al.* (2004) and Choe *et al.* (2008). The average yearly temperature to evaluate the stiffening of bearing pad for bridges located in SC are 66°F –almost 10°F higher than TN where deicing salt exposure was considered.

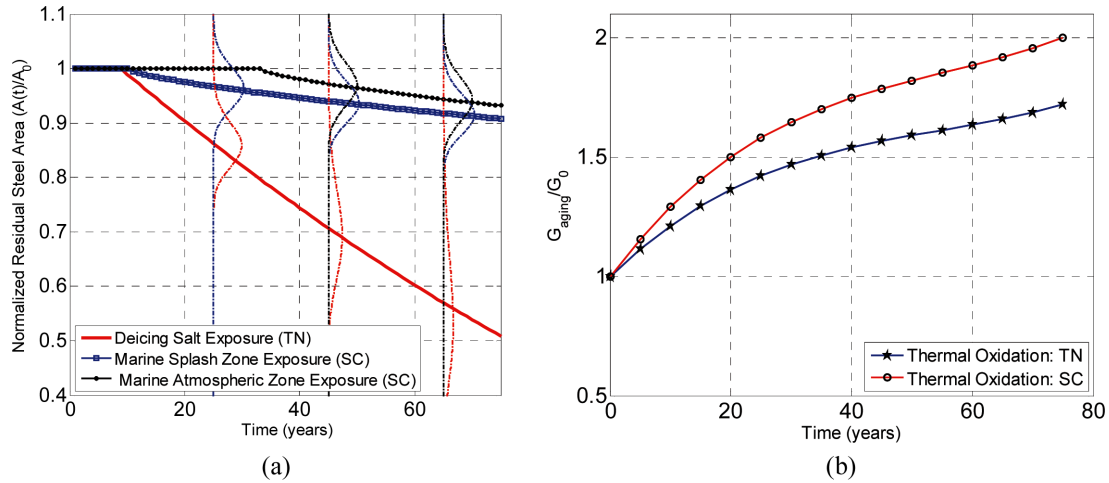


Fig. 7 (a) Normalized residual area of column reinforcement under different exposure conditions and (b) variation of stiffness modulus change due to thermal oxidation in Tennessee and South Carolina

Fig. 7 shows the normalized area reduction of steel and increase in shear modulus of elastomeric bearing pads under the different exposure conditions and bridge locations. It can be observed that for the same reinforcement layout and cover depth in the RC columns, deicing salt exposure leads to the shortest expected corrosion initiation time (approximately 8 years) and also results in significantly higher cross sectional area loss of steel as compared to either marine splash zone or atmospheric chloride exposure. Also, both sources of marine chloride degradation lead to a lesser uncertainty about the mean area loss of steel, relative to the deicing salt exposure. A similar trend is observed for the cross sectional area loss of steel dowels in the bridge bearings under different exposure conditions. Additionally a higher average annual temperature in SC is found to result in further stiffening of the neoprene rubber pad in bridge bearings as compared to TN. Another interesting observation is that for the atmospheric zone exposure, the onset of corrosion to reinforcing steel in concrete is found to be significantly delayed relative to the other exposure conditions. Hence the impact on seismic fragility under chloride exposure from atmospheric marine zone is expected to be solely due to stiffening of the bearing pad for the initial period in the bridge's service life.

Comparisons of the seismic fragility of the bridge class under different exposure conditions are presented in Fig. 8, which shows several interesting observations. For instance, Figs. 8(a) and (b) depict the change in bridge system fragility for the moderate damage state under sea-splash and atmospheric chlorides exposure at different points in time in the service life. Although both exposure conditions clearly reveal that towards the end of service life (75 years) both exposure conditions render the bridge more vulnerable to seismic threats, the variation in bridge fragility due to aging is quite insignificant especially for the case of marine atmospheric exposure. This phenomenon is primarily because while corrosion deterioration of RC columns tends to render the bridge more fragile, stiffening of the elastomeric bearing pads is beneficial to bridge behavior by reducing bearing displacement, as elaborated in Section 4.2. Consequently, for an extended period along the service life of the bridge, it is not possible to single out the dominant of the two deterioration mechanisms discussed above. However, towards the end of the service period, column

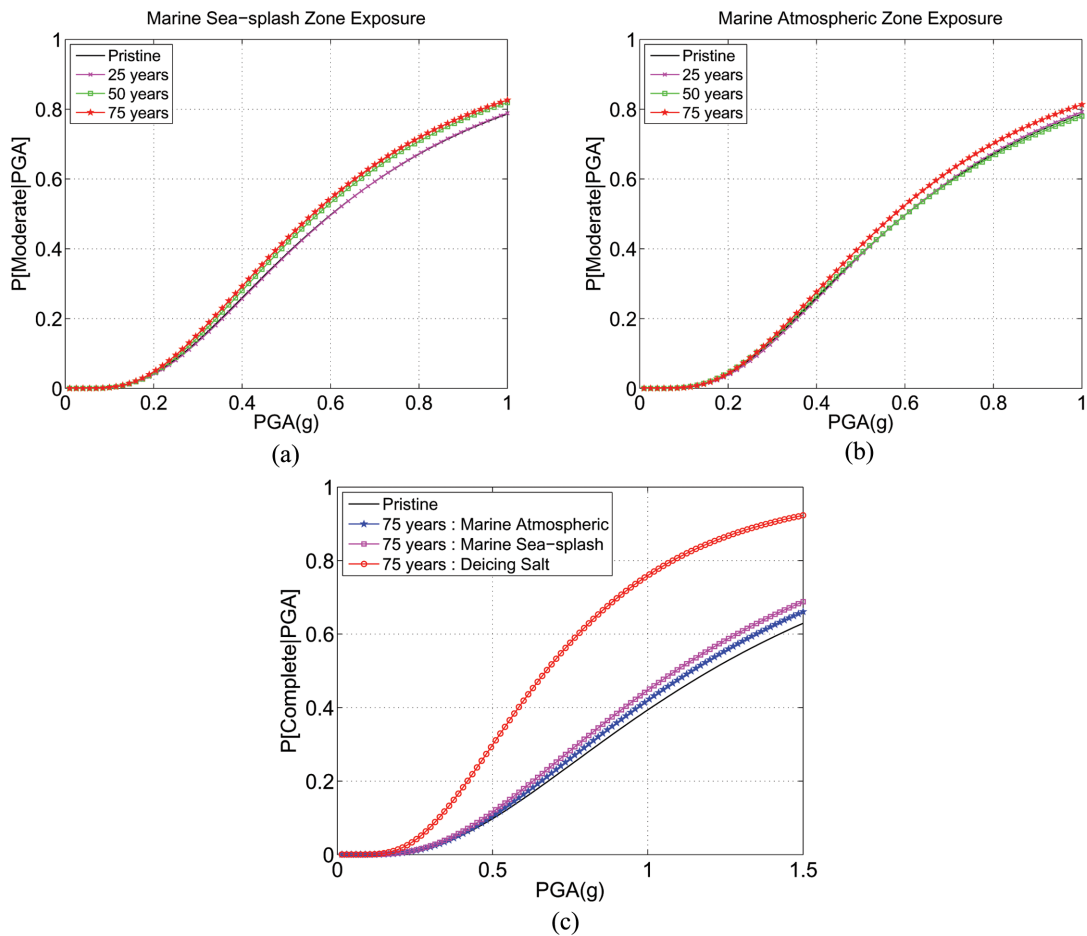


Fig. 8 (a) Aging bridge seismic fragility curves for moderate damage state under sea-splash exposure, (b) aging bridge seismic fragility curves for moderate damage state under atmospheric exposure and (c) comparison of fragility curves for the complete damage state under different exposure conditions

deterioration dominates as revealed by a clear increase in bridge fragility at 75 years. A comparison between Figs. 8(a) and (b) also shows that marine sea splash exposure is more detrimental to bridge fragility because of higher loss of steel area due to corrosion as compared to atmospheric conditions. A comparison of the impact of all three different exposure conditions on bridge fragility is shown in Fig. 8(c) for the complete damage state. This figure clearly shows the relative comparison of the impact of severity of the three distinct exposure conditions considered in this study. The median values for the fragility curves for the atmospheric, sea-splash and deicing salt exposure are found to be 5%, 9% and 44% lesser than the median value for the as-built pristine bridge fragility. These findings highlight that while atmospheric chloride exposure has the least impact on seismic fragility of aging bridges, exposure to chlorides stemming from deicing salt exposure is most detrimental. This high level of deterioration associated with chloride ions stemming from deicing salt exposure as compared to other exposure conditions have also been validated in the past by Stewart and Rosowsky (1998) with respect to live load reliability of

concrete bridges. The deteriorated fragility estimates for different exposure conditions can also be used to assess the annual probability of exceeding various damage states after integration with the site specific seismic hazard curve. These exceedance probabilities offer further insight into the relative importance of acknowledging deterioration during exposure to seismic hazards, by incorporating the likelihood of exceeding various ground motion PGA levels at the bridge site. In order to have a comparative estimate of effect of deterioration on the annual probability of damage state exceedance, the hazard curve for Nutbush, TN is adopted (USGS 2011). Relative to a pristine bridge, the results reveal a 6%, 14% and 96% increase in annual probability of exceeding complete damage for the atmospheric, sea-splash and deicing salt exposure conditions, respectively. Such results show the impact of accounting for the effects of aging and deterioration while calculating region specific seismic risks. Additionally, Ghosh and Padgett (2011) also revealed the importance of incorporating lifetime degradation of bridge structures in order to determine life-cycle cost estimates.

With the wealth of information available with respect to time-evolving fragility curves for MSSS concrete bridge classes under different exposure conditions, there is an underlying need to propose techniques that help to quickly assess bridge vulnerability at any point in time in the service life. This is achieved in this study by proposing time dependent scaling factors to modify the median and dispersion values, hence offering an efficient way to quantify and conveniently express decrease in bridge reliability over time. Consequently, unique time dependent scaling factors are required for the median and dispersion values for different damage states and can be calculated using time dependent polynomial regression functions. In this study three parameter quadratic regression functions of the form shown in Eq. (17) are adopted for this purpose.

$$\text{Scaling factor } (t) = x_1 t^2 + x_2 t + x_3 \quad (17)$$

where, and x_1 , x_2 and x_3 are the quadratic coefficients of the regression analysis. In the context of aging MSSS concrete bridge classes, Table 3 shows a set of unique scaling factors for the median and dispersion values corresponding to different damage states and exposure conditions.

The seismic fragility parameters ($med_{sys}(t)$ and $disp_{sys}(t)$) of a t year old bridge as presented in Eq. (16) can be directly calculated as

$$\text{Fragility Parameter } (t) = \text{Scaling factor } (t) * \text{Fragility parameter } (t=) \quad (18)$$

Fragility parameters for the pristine bridge corresponding to the last term of Eq. (18) for different damage states are presented in Table 4. If now, for instance, it is required to calculate the median value of fragility corresponding to extensive damage state for a 40 year old bridge under deicing salt exposure, it is simply a product of scaling factor 0.79 (obtained using Table 3) and the median value of the pristine bridge 0.87 (obtained using Table 4). The dispersion value for the same 40 year old bridge can also be calculated accordingly using the same procedure. The proposed scaling factors can help to evaluate time dependent bridge failure probabilities without the need to carry out a full new fragility analysis at each time period for similar multiple span concrete girder bridges. Such factors can be easily incorporated in regional risk assessment software and used by bridge owners, transportation departments and managers for regional risk assessment of portfolio of structures with geometric variations and different chloride exposure conditions.

Table 3 Coefficients of the quadratic scaling factors for fragility parameters for different damage states and exposure conditions

Fragility parameter	Deicing salt exposure			Sea-splash zone exposure			Atmospheric zone exposure		
	x_1	x_2	x_3	x_1	x_2	x_3	x_1	x_2	x_3
Median (PGA)									
Slight	$-4.0E-05$	$1.8E-03$	1	$-5.0E-05$	$4.9E-03$	1	$-4.6E-05$	$4.6E-03$	1
Moderate	$-1.0E-05$	$-4.0E-03$	1	$-8.6E-06$	$-4.2E-04$	1	$-1.8E-05$	$8.3E-04$	1
Extensive	$9.2E-07$	$-5.3E-03$	1	$-2.3E-05$	$4.5E-04$	1	$-2.6E-05$	$1.5E-03$	1
Complete	$3.3E-06$	$-6.2E-03$	1	$-3.1E-05$	$9.1E-04$	1	$-3.4E-05$	$2.1E-03$	1
Dispersion (PGA)									
Slight	$-2.8E-05$	$4.7E-05$	1	$-7.0E-06$	$-2.3E-05$	1	$-1.3E-05$	$4.6E-04$	1
Moderate	$-1.2E-05$	$-1.2E-03$	1	$7.5E-06$	$-1.0E-03$	1	$-1.3E-05$	$8.1E-04$	1
Extensive	$-4.3E-06$	$-1.5E-03$	1	$-3.6E-06$	$-3.5E-04$	1	$-1.6E-05$	$1.1E-03$	1
Complete	$-1.1E-05$	$-1.4E-03$	1	$-1.8E-06$	$-4.6E-04$	1	$-1.7E-05$	$1.1E-03$	1

Table 4 Fragility parameters corresponding to the pristine MSSS concrete bridge class under different exposure conditions

Slight damage		Moderate damage		Extensive damage		Complete damage	
$*med_{sys}(0)$	$*disp_{sys}(0)$	$*med_{sys}(0)$	$*disp_{sys}(0)$	$*med_{sys}(0)$	$*disp_{sys}(0)$	$*med_{sys}(0)$	$*disp_{sys}(0)$
0.208	0.687	0.603	0.637	0.869	0.657	1.201	0.676

$*med_{sys}(0)$ = Median value of fragility corresponding to pristine bridge, $*disp_{sys}(0)$ = Median value of fragility corresponding to pristine bridge.

6. Conclusions

Seismic vulnerability modeling of highway bridges has typically neglected the time-dependent effects of aging when quantifying the seismic fragility, or conditional probability of failure. Recent insights on the importance of considering the joint effects of aging and seismic hazards have yet to address several key aspects in the fragility analysis. This paper addresses such deficiencies by accounting for:

- (1) Deterioration mechanisms of multiple critical bridge components typical of concrete bridges
- (2) Uncertainty in bridge geometry for seismic fragility analysis of aging bridge classes in addition to variations in material, modeling and deterioration parameters
- (3) Assessment of the impact of severity of three different environmental exposure conditions on seismic fragility of aging bridges.

The approach can be emulated to assess the time-dependent fragility of other aging bridge classes, provides new insight on the relative importance of multiple component deterioration and exposure condition for aging reinforced concrete bridges, and provides fragility scaling factors that can be directly adopted in regional seismic risk assessment of aging bridges.

This study shows that including the effects of corrosion deterioration of reinforced concrete columns alone is not enough to evaluate the important changes in seismic fragility of aging RC

bridges. Cross-sectional area reduction of dowel bars and stiffening of the elastomeric bearing pads are also found to have a pronounced effect on deteriorating bridge vulnerability. Based on the probabilistic seismic demand analysis conducted in this study, it is found that when deterioration mechanisms of different bridge components are considered together they may result in significant increase in seismic demand of some bridge components such as the curvature ductility of bridge columns. For some components, such as fixed bearings in the longitudinal direction, joint consideration of deterioration mechanisms have negligible impacts on the demand relative to the case when only bearing deterioration is considered.

From the detailed component fragility analysis under the deicing salt exposure condition, some components such as columns show a constant decrease in median values (hence an increase in seismic fragility) along the service life of the bridge. Other components, for instance expansion bearings in the transverse direction, show an initial increase followed by a rapid decrease in fragility. This can be attributed to complex dynamic behavior of the aging bridge system and its components. For the MSSS concrete girder bridge the bearing pad stiffening has a predominant influence on component fragility over loss of steel area in bearing dowels or column reinforcement during the initial period of service life. However, for all damage states and components, the fragility curves reveal an increase in vulnerability after approximately 33 years of exposure. For the deicing salt and sea splash zone, an increase in seismic vulnerability was observed much earlier at 8 years and 10 years respectively corresponding to the corrosion initiation time and subsequent area loss of steel in RC columns. Furthermore, development of joint probabilistic seismic demand models and assessment of bridge system fragility reveal that under deicing salt exposure conditions the bridge as a whole becomes increasingly more vulnerable due to aging and deterioration. Hence even amidst variation in bridge geometry and other modeling parameters, this study shows that the effects of component deterioration are critical considerations when assessing the fragility of aging bridge classes.

In addition to deicing salt exposure, the other deterioration mechanisms considered are chlorides stemming from exposure to sea-splash zone and atmospheric zone with regard to marine exposure. It is found that for the sea-splash zone the bridge system fragility also continues to increase with age, however, the increase in fragility is not as dramatic as deicing salt exposure. For the atmospheric exposure however an interesting trend is observed. It is found that stiffening of the bearing pad and no initial deterioration of the columns and bearings dowels tends to make the bridge less vulnerable than the pristine state for the initial period. As degradation effects of dowels and rebars in columns set in, the bridge fragility steadily increases. At the end of the bridge's service life (75 years) the varied impact of the three exposure scenarios on the susceptibility to complete damage is distinct. The results of the study show that median values for the fragility curves for the atmospheric, sea-splash and deicing salt exposure are found to be 5%, 9% and 44% lesser than the median value corresponding to the pristine bridge fragility. These results underline the importance of considering corresponding exposure condition while assessing seismic fragility of classes of aging reinforced concrete bridges. Lastly, quadratic scaling factors are presented to evaluate changes in time dependent bridge fragility parameters along the service life, relative to as-built or pristine fragility parameters for multiple span concrete girder bridge classes. Such scaling factors provide a simple approach to estimate the present day bridge vulnerability depending on the age and exposure condition and can be used to support risk assessment and mitigation planning for regional bridge infrastructure in locations prone to chloride exposure.

Acknowledgements

The authors gratefully acknowledge the support from the National Science Foundation through grant CMMI-0928493.

References

- Akgul, F. and Frangopol, Dan M. (2004), "Lifetime performance analysis of existing prestressed concrete bridge superstructures", *J. Struct. Eng.-ASCE*, **130**(12), 1889-1903.
- Almusallam, A.A. (2001), "Effect of degree of corrosion on the properties of reinforcing steel bars", *Constr. Build. Mater.*, **15**(8), 361-368.
- Aquino, W. and Hawkins, N.M. (2007), "Seismic retrofitting of corroded reinforced concrete columns using carbon composites", *ACI Struct. J.*, **104**(3), 348-356.
- Basoz, N. and Kiremidjian, A.S. (1999), "Development of empirical fragility curves for bridges", *Technical Council on Lifeline Earthquake Engineering Monograph*, (16), 693-702.
- Bertolini, L., Elsener, B., Pedferri, P. and Polder, R.B. (2004), *Corrosion of steel in concrete: prevention, diagnosis, repair*, Wiley-VCH.
- Choe, D.E., Gardoni, P., Rosowsky, D. and Haukaas, T. (2008), "Probabilistic capacity models and seismic fragility estimates for RC columns subject to corrosion", *Reliab. Eng. Syst. Safe.*, **93**(3), 383-393.
- Choe, D.E., Gardoni, P., Rosowsky, D. and Haukaas, T. (2009), "Seismic fragility estimates for reinforced concrete bridges subject to corrosion", *Struct. Saf.*, **31**(4), 275-283.
- Choi, E. (2002), "Seismic analysis and retrofit of Mid-America bridges", PhD Thesis, Georgia Institute of Technology, Atlanta, Georgia.
- Choi, E., DesRoches, R. and Nielson, B. (2004), "Seismic fragility of typical bridges in moderate seismic zones", *Eng. Struct.*, **26**(2), 187-199.
- Cornell, C.A., Jalayer, F., Hamburger, R.O. and Foutch, D.A. (2002), "Probabilistic basis for 2000 SAC federal emergency management agency steel moment frame guidelines", *J. Struct. Eng.*, **128**(4), 526-533.
- Davis, J.R. (2000), *Corrosion: understanding the basics*, ASM International.
- Duracrete (2000), *Probabilistic performance based durability design of concrete structures: Final technical report*, The European Union - Brite EuRam III.
- Enright, M.P. and Frangopol, Dan M. (1998), "Probabilistic analysis of resistance degradation of reinforced concrete bridge beams under corrosion", *Eng. Struct.*, **20**(11), 960-971.
- Fang, C., Lundgren, K., Chen, L. and Zhu, C. (2004), "Corrosion influence on bond in reinforced concrete", *Cement Concrete Res.*, **34**(11), 2159-2167.
- FHWA. (2009), "FHWA bridge programs NBI data", <http://www.fhwa.dot.gov/bridge/britab.cfm>.
- Frangopol, D.M., Kai-Yung, Lin and Estes, A.C. (1997), "Reliability of reinforced concrete girders under corrosion attack", *J. Struct. Eng.-ASCE*, **123**(3), 286-297.
- Ghosh, J. and Padgett, J. (2010), "Aging considerations in the development of time-dependent seismic fragility curves", *J. Struct. Eng.*, **136**(12), 1497-1511.
- Ghosh, J. and Padgett, J.E. (2011), "Probabilistic seismic loss assessment of aging bridges using a component level cost estimation approach", *Earthq. Eng. Struct. D.*, **40**(15), 1743-1761.
- Hoffman, Paul C. and Weyers, Richard E. (1996), "Probabilistic durability analysis of reinforced concrete bridge decks", *Proceedings of the 1996 7th Specialty Conference on Probabilistic Mechanics and Structural Reliability*, ASCE, Worcester, MA, USA, 290-293.
- Imbsen, R.A. and Nutt, R.V. (1981), "Increased seismic resistance of highway bridges using improved bearing design concepts", *Dynamic Response of Structures, Experimentation, Observation, Prediction, and Control*, ASCE, New York, NY, 416-430.
- Itoh, Y. and Gu, H.S. (2009a), "Prediction of aging characteristics in natural rubber bearings used in bridges", *J. Bridge Eng.*, **14**(2), 122-128.
- Itoh, Y. and Gu, H.S. (2009b), "Prediction of aging characteristics in natural rubber bearings used in bridges", *J.*

- Bridge Eng.*, **14**(2), 122-128.
- Itoh, Y., Gu, H., Satoh, K. and Kutsuna, Y. (2006), "Experimental investigation on ageing behaviors of rubbers used for bridge bearings", *Struct. Eng. Earthq. Eng.*, **23**(1), 17-31.
- Kelly, J.M. (1997), *Earthquake-resistant design with rubber*, Springer.
- Le Huy, M. and Evrard, G. (1998), "Methodologies for lifetime predictions of rubber using Arrhenius and WLF models", *Die Angewandte Makromolekulare Chemie*, **261-262**(1), 135-142.
- Lindquist, L. (2008), "Corrosion of steel bridge girder anchor bolts", MS Thesis, Georgia Institute of Technology, Atlanta, Georgia.
- Liu, C. (2005), "Evolutionary multiobjective optimization in engineering management: An empirical study on bridge deck rehabilitation", *6th International Conference on Parallel and Distributed Computing, Applications and Technologies*, PDCAT 2005, December 5, 2005 - December 8, 2005, Institute of Electrical and Electronics Engineers Computer Society, Dalian, China, 773-777.
- Mase, G.T. and Mase, G.E. (1999), *Continuum mechanics for engineers*, CRC Press.
- Maslehuddin, M., Allam, I.A., Al-Sulaimani, G.J., Al-Mana, A. and Abduljauwad, S.N. (1990), "Effect of rusting of reinforcing steel on its mechanical properties and bond with concrete", *ACI Mater. J.*, **87**(5), 496-502.
- Mazzoni, S., McKenna, F., Scott, M.H. and Fenves, G.L. (2009), *OpenSees command language manual*, Command Language Manual, University of California, Berkeley.
- Melchers, Robert E. and Frangopol, Dan M. (2008), "Probabilistic modelling of structural degradation", *Reliab. Eng. Syst. Safe.*, **93**(3), 363.
- Nielson, B.G. (2005), "Analytical fragility curves for highway bridges in moderate seismic zones", PhD Thesis, Georgia Institute of Technology, Atlanta, Georgia.
- Nielson, B.G. and DesRoches, R. (2007), "Analytical seismic fragility curves for typical bridges in the Central and Southeastern United States", *Earthq. Spectra*, **23**(3), 615-633.
- Nielson, Bryant G. and DesRoches, R. (2007), "Seismic fragility methodology for highway bridges using a component level approach", *Earthq. Eng. Struct. D.*, **36**(6), 823-839.
- NOAA (National Oceanic and Atmospheric Administration). (2004), "Climatology of the United States", http://cdo.ncdc.noaa.gov/climate_normals/clim20/tn/406402.pdf.
- Padgett, J.E. and DesRoches, R. (2007), "Bridge functionality relationships for improved seismic risk assessment of transportation networks", *Earthq. Spectra*, **23**(1), 115-130.
- Padgett, J.E. and DesRoches, R. (2008), "Methodology for the development of analytical fragility curves for retrofitted bridges", *Earthq. Eng. Struct. D.*, **37**(8), 1157-1174.
- Rix, G.J. and Fernandez, J.A. (2004), "Earthquake ground motion simulation", www.ce.gatech.edu/research/mae_ground_motion/.
- Shinozuka, M., Feng, M.Q., Lee, J. and Naganuma, T. (2000), "Statistical analysis of fragility curves", *J. Eng. Mech.-ASCE*, **126**(12), 1224-1231.
- Silano, L.G. and Brinckerhoff, P. (1993), *Bridge inspection and rehabilitation*, Wiley-IEEE.
- Stewart, Mark G. and Rosowsky, D.V. (1998), "Time-dependent reliability of deteriorating reinforced concrete bridge decks", *Struct. Saf.*, **20**(1), 91-109.
- superstructures", *J. Struct. Eng.-ASCE*, **130**(12), 1889-1903.
- Thoft-Christensen, P., Jensen, F.M., Middleton, C.R. and Blackmore, A. (1996), "Assessment of the reliability of concrete slab bridges", Conference or Workshop Item, <http://publications.eng.cam.ac.uk/6361/>.
- USDOS (U.S. Department of State). (2010), "US weather - Average temperatures and rainfall", <http://countrystudies.us/united-states/weather/>.
- USGS (2011), "Hazards: Seismic hazard maps and data", Earthquake hazards program, <http://earthquake.usgs.gov/hazards/>.
- Val, D.V., Stewart, M.G. and Melchers, R.E. (2000), "Life-cycle performance of RC bridges: Probabilistic approach", *Comput. Aided Civil Infrastruct. Eng.*, **15**(1), 14-25.
- Vu, K.A.T. and Stewart, Mark G. (2000), "Structural reliability of concrete bridges including improved chloride-induced corrosion models", *Struct. Saf.*, **22**(4), 313-333.
- Wen, Y.K. and Wu, C.L. (2001), "Uniform hazard ground motions for Mid-America cities", *Earthq. Spectra*, **17**(2), 359-384.
- Weyers, R.E., Fitch, M.G., Larsen, E.P., Al-Qadi, I.L. and Hoffman, P.C. (1994), *Concrete bridge protection and*

- rehabilitation: Chemical and physical techniques, Service Life Estimates*, Strategic Highway Research Program, Washington D.C.
- Whiting, D., Stejskal, B. and Nagi, M. (1990), *Condition of prestressed concrete bridge components: technology review and field surveys*, Federal Highway Administration, Washington.
- Wright, T., DesRoches, R. and Padgett, J.E. (2011), "Bridge seismic retrofitting practices in the Central and Southeastern United States", *J. Bridge Eng.*, **16**(1), 82-92.
- Yokozaki, K., Motohashi, K., Okada, K. and Tsutsumi, K. (1997), "A rational model to predict the service life of RC structures in marine environment, Forth CANMET", *ACI International Conference on Durability of Concrete*, 777-799.
- Zhong, J., Gardoni, P. and Rosowsky, D. (2011), "Seismic fragility estimates for corroding reinforced concrete bridges", *Struct. Infrastruct. Eng.*, **8**(1), 55-69.

CC

Appendix

The capacity limit states adopted for each bridge component are listed in Table A1. Table shows median and dispersion values of the lognormally distributed component capacities.

Table A1 Capacity limit states for different bridge components for the multiple span simply supported concrete girder bridge class obtained after statistical combination of experimental results and expert judgment (adapted from Nielson and DesRoches 2007a)

Component	Units	Slight		Moderate		Extensive		Complete	
		S_c	β_c	S_c	β_c	S_c	β_c	S_c	β_c
Concrete columns	--	1.29	0.59	2.10	0.51	3.52	0.64	5.24	0.65
Fixed bearings - Longitudinal	mm	28.9	0.60	104.2	0.55	136.1	0.59	186.6	0.65
Fixed bearings - Transverse	mm	28.8	0.79	90.9	0.68	142.2	0.73	195.0	0.66
Expansion bearings - Longitudinal	mm	28.9	0.60	104.2	0.55	136.1	0.59	186.6	0.65
Expansion bearings - Transverse	mm	28.8	0.79	90.9	0.68	142.2	0.73	195.0	0.66
Abutment - Passive	mm	37.0	0.46	146.0	0.46	<i>N/A</i>	<i>N/A</i>	<i>N/A</i>	<i>N/A</i>
Abutment - Active	mm	9.8	0.70	37.9	0.90	77.2	0.85	<i>N/A</i>	<i>N/A</i>
Abutment - Transverse	mm	9.8	0.70	37.9	0.90	77.2	0.85	<i>N/A</i>	<i>N/A</i>